



# **An investigation of structure and electrical characteristics of lanthanum strontium manganite nanopowders with different Sr 2+ ion concentrations**

Ali Omar Turkey, Mohamed Mohamed Rashad, Ali Mostafa Hassan, Elsayed Elnaggar, Mikhael Bechelany

## **► To cite this version:**

Ali Omar Turkey, Mohamed Mohamed Rashad, Ali Mostafa Hassan, Elsayed Elnaggar, Mikhael Bechelany. An investigation of structure and electrical characteristics of lanthanum strontium manganite nanopowders with different Sr 2+ ion concentrations. Particulate Science and Technology, 2017, 36 (7), pp.873 - 877. <10.1080/02726351.2017.1313798>. <hal-01812131>

**HAL Id: hal-01812131**

**<https://hal.science/hal-01812131v1>**

Submitted on 4 Jun 2021

**HAL** is a multi-disciplinary open access archive for the deposit and dissemination of scientific research documents, whether they are published or not. The documents may come from teaching and research institutions in France or abroad, or from public or private research centers.

L'archive ouverte pluridisciplinaire **HAL**, est destinée au dépôt et à la diffusion de documents scientifiques de niveau recherche, publiés ou non, émanant des établissements d'enseignement et de recherche français ou étrangers, des laboratoires publics ou privés.



HAL Authorization

# **An Investigation of Structure and Electrical Characteristics of Lanthanum Strontium Manganite (LSM) Nanopowders with Different $\text{Sr}^{2+}$ Ion Concentrations**

Ali Omar Turkey

Central Metallurgical Research & Development Institute, Helwan, Cairo, Egypt

Department of Inorganic Nonmetallic Materials, University of Science and Technology Beijing,  
Beijing, China

Institut Européen des Membranes, Université de Montpellier, Montpellier, France

Mohamed Mohamed Rashad

Central Metallurgical Research & Development Institute, Helwan, Cairo, Egypt

Ali Mostafa Hassan

Faculty of Science, Chemistry department, Al-Azhar University, Nasar City, Egypt

Elsayed M. Elnaggar

Faculty of Science, Chemistry department, Al-Azhar University, Nasar City, Egypt

Mikhael Bechelany

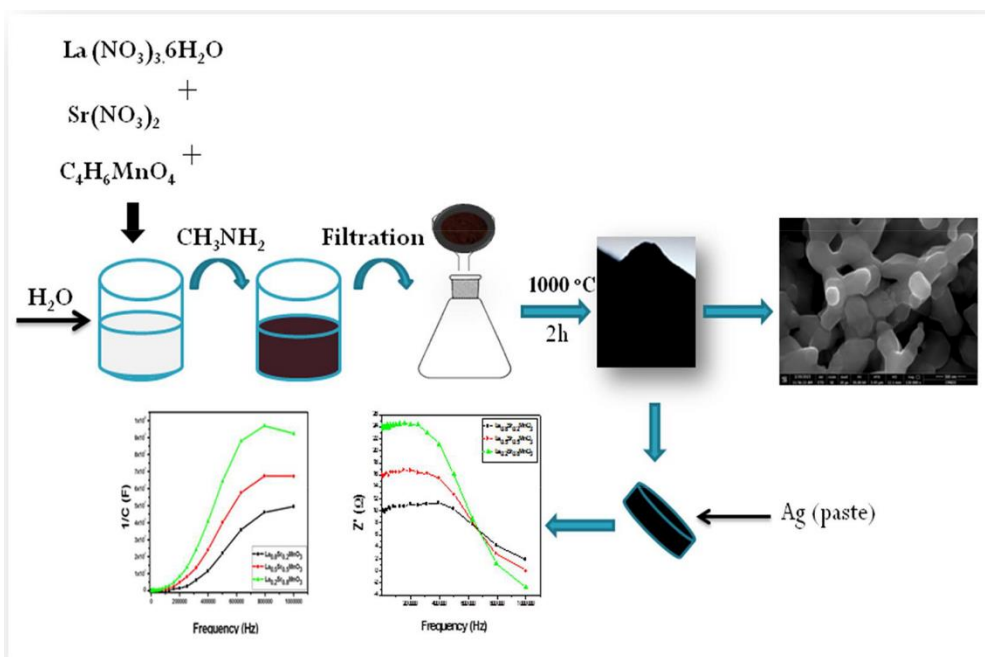
Institut Européen des Membranes, Université de Montpellier, Montpellier, France

Address correspondence to Ali Omar Turkey. Email: ali\_omar155@yahoo.com

## **Abstract**

Generally, the efficiency of solid oxide fuel cells (SOFCs) is heavily dependent on the electrocatalytic activity of the cathode toward the oxygen reduction reaction (ORR). In order to achieve a better cathode performance,  $\text{La}_x\text{Sr}_{1-x}\text{MnO}_3$  (LSM) nanopowders with different  $\text{Sr}^{2+}$  ion contents varying from 0.2 to 0.8 have been synthesized using the co-precipitation method. The obtained nanoparticles were characterized by X-ray diffraction (XRD), field emission scanning electron microscopy (FESEM) and electrochemical impedance spectroscopy (EIS). It is found that the LSM nanoparticles were seemed to exhibit the high polarization resistance with the increase of the  $\text{Sr}^{2+}$  ion molar ratios. The crystallite size was found to increase from 16.4 to 24.3 nm with increasing the  $\text{Sr}^{2+}$  content from 0.2 to 0.8. The lattice parameters were decreased with  $\text{Sr}^{2+}$  ion content which may be caused by an increase in internal stress with increasing the grain size of LSM. Meanwhile, the real part impedance ( $Z'$ ) was increased from 10( $\Omega$ ) at 0.2  $\text{Sr}^{2+}$  to be 24( $\Omega$ ) at 0.8  $\text{Sr}^{2+}$  ion ratio. Alternatively,  $|Z|$  of prepared sample was increased from 12 to 26 ( $\Omega$ ) by increasing  $\text{Sr}^{2+}$  ion molar ratios from 0.2 to 0.8.

### Graphical abstract



**Keywords:** co-precipitation method, electrochemical impedance spectroscopy, LSM, SOFCs

## 1 INTRODUCTION

Newly, there has been considerable interest in the synthesis and the growth of the perovskite oxides with  $ABO_3$  structure and their use as a cathode for solid oxide fuel cell (SOFCs) (Huang, Vohs, and Gorte 2005). Among them, strontium substituted lanthanum manganite (LSM) has been act as one of the most notable and functional members of the perovskite family cathode materials due to its phenomenal electrochemical movement for oxygen reduction as well as its thermal and chemical compatibility with yttria stabilized zirconia (YSZ). Accordingly, different studies have been implemented in order to explore the impact of  $Sr^{2+}$  doping and the terminal morphology on its electrochemical activity. However, the cathode material is still the limiting ingredient to make a further step forward. Reducing the operating temperature leads to constringe of the catalytic activity of the cathode for oxygen reduction

process (Liang et al. 2009). Subsequently, in the case of classical strontium-doped lanthanum manganite (LSM), the high p-type electronic conductivity arises from the presence of mixed valence Mn ( $\text{Mn}^{3+}$  and  $\text{Mn}^{4+}$ ), which is enhanced by doping with  $\text{Sr}^{2+}$  ion. This doping allows LSM to have a potential application in the electro-catalysts because of its high stability, good catalytic activity toward oxygen reduction reaction, and excellent compatibility with the yttria-stabilized zirconia (YSZ) electrolyte (Jorgensen and Mogensen 2001; Sholklapper et al. 2007; Orera and Slater 2010; Liu et al. 2013; Ju et al. 2016). LSM has good electronic conductivity but possesses poor ionic conductivity. For this reason, most of the oxygen reduction reaction occurs at the triple phase boundaries of the electrode/electrolyte/gas phase (Wang et al. 2009; Im, Park, and Shin 2011; Turkey et al. 2015) although LSM is predominantly an electronic conductor ( $200 \text{ S cm}^{-1}$ ) (Yan et al. 2014; Reshi et al. 2015). Consequently, synthesis of LSM has been extensively studied using different strategies including organic acid precursors, mechanochemical, solid state and co-precipitation methods (Yang and Irvine 2008; Zhi et al. 2011; Lu et al. 2015; Turkey, Rashad, and Bechelany). Co-precipitation method is found to be the most popular technique for mass production with low cost, narrow size distribution and uniform microstructure. In this context, LSM powder was synthesized through the carbonate co-precipitation method as described by Turkey et al. (2016), (Cesario et al. 2011). Alternatively, one of the serious drawbacks of the method was the incorporation of  $\text{Na}^+$  ions in the precipitate which decrease the efficiency of LSM as a cathode material. Therefore, herein, the objective of this work is to synthesize and to tune the crystal structure and the electrical properties ( $Z'$ ,  $Z''$ ,  $I/C$  and  $I/C^2$ ) of  $\text{La}_{1-x}\text{Sr}_x\text{MnO}_3$  with different concentrations ( $x = 0.2, 0.5, 0.8$ ) using the co-precipitation method based on methyl amine as a base at pH 12. Methyl amine has been used for the first time as a base in the synthesis of lanthanum strontium manganite. Effort was made first

to demonstrate the change in the structural properties. Meanwhile, the impact of substituting Sr on the electrical properties was investigated.

## 2 MATERIALS AND METHODS

### 2.1 Materials

All the chemicals used in this study such as lanthanum nitrate hexahydrate  $\text{La}(\text{NO}_3)_3 \cdot 6\text{H}_2\text{O}$  Fluka Analytical, anhydrous strontium nitrate  $\text{Sr}(\text{NO}_3)_2$  (Sigma-Aldrich), manganese acetate tetrahydrate  $\text{C}_4\text{H}_6\text{MnO}_4$  (AppliChem), and methylamine ( $\text{CH}_3\text{NH}_2$ ) were used as received. Moreover, deionized water was used in the whole work.

### 2.2 Procedure

Lanthanum strontium manganite (LSM) nanopowders were synthesized through co-precipitation route by mixing aqueous solutions of lanthanum nitrate hexahydrate  $\text{La}(\text{NO}_3)_3 \cdot 6\text{H}_2\text{O}$ , strontium nitrate  $\text{Sr}(\text{NO}_3)_2$  and manganese acetate tetrahydrate ( $\text{C}_4\text{H}_6\text{MnO}_4$ ). Methylamine was added as a base to the mixture till that the solution reached a  $pH$  of 12. The mixture solution was gently stirred, filtrated, washed and dried. The products were ground and annealed in pure alumina crucibles at '1000°C' for '2 h' in a muffle furnace (under air) with '10°C'/min heating rate in order to achieve the corresponding perovskite structure.

### 2.3 Physical Characterization

X-ray powder diffraction (XRD) was carried out on a model Bruker AXS diffractometer (D8-ADVANCE Germany) with  $\text{Cu } K\alpha$  ( $\lambda = 1.54056 \text{ \AA}$ ) radiation, operating at 40kV and 40mA. The diffraction data were recorded for  $2\theta$  values between 10 and 80°. Field emission scanning electron microscopy was performed by a FE-SEM (JEOL-JSM-5410 Japan). All impedance

spectroscopy spectra were recorded with 6 points pr. decade with an AC perturbation signal of 50mA using a PARSTAT 4000 Potentiostat/Galvanostat/EIS Analyzer. The impedance spectra were recorded with two frequency ranges.

## 3 RESULTS AND DISCUSSION

### 3.1 Crystal Structure

**Figure 1** indicates the XRD patterns of the  $\text{La}_{1-x}\text{Sr}_x\text{MnO}_3$  samples at different  $\text{Sr}^{2+}$  ratios prepared by co-precipitation route using methylamine as a base then calcined at ‘1000°C’ for ‘2h’. The main peak of the perovskite lanthanum strontium manganite LSM nanopowders at  $\sim 33^\circ$  is matched for all synthesized samples. Monoclinic perovskite like structure of LSM ( $a = 5.4712$ ,  $b = 7.7716$ ,  $c = 5.5031$  (Å) and the space-group  $P21/a$ ) was detected as crystalline form for all samples which is in agreement with (JCPDS # 049-0595). It is clear that the samples with high  $\text{Sr}^{2+}$  ion concentrations exhibited a small shift in the XRD peaks towards a larger  $2\theta$ . The shift was increased with increasing  $\text{Sr}^{2+}$  ion content as the result of a decrease of the distances between the crystalline planes. It is clear that the change of  $\text{Sr}^{2+}$  ion ratio gave a detectable change in the lattice parameters. Of note, the lattice parameters were found to slightly reduce from ( $a = 5.5212$ ,  $b = 7.8712$ ,  $c = 5.6421$ ) Å for  $x = 0.2$  to ( $a = 5.5201$ ,  $b = 7.8201$ ,  $c = 5.6400$ ) Å for  $x = 0.8$  as the result of the increase in internal stress with increasing the grain size of LSM. Meanwhile, the unit cell volume  $V_{\text{cell}}$  was decreased from 245.197 to 243.466 Å<sup>3</sup>, as shown in **Table 1**. Patently, the crystallite size was  $\text{Sr}^{2+}$  ion dependent. In this context, it was increased with further increasing of  $\text{Sr}^{2+}$  ion content. The substitution of  $\text{La}^{3+}$  cation (1.36 Å) by a larger one  $\text{Sr}^{2+}$  (1.44 Å) led to the progressive increase in the number of holes from  $\text{Mn}^{3+}$  to  $\text{Mn}^{4+}$ . Subsequently, the substitution of La 3p by Sr 2p increases the content of  $\text{Mn}^{4+}$  ions to keep the

charge neutrality (Kakade, Ramanathan, and De 2003; Marinsek et al. 2007). Furthermore, the crystalline phases of  $\text{La}_{1-x}\text{Sr}_x\text{MnO}_3$  are segregated upon an increase in  $\text{Sr}^{2+}$  concentration. A small splitting of the main peak of the perovskite at  $\sim 33^\circ$ , which is an indication of a monoclinic system, is observed in the XRD pattern. The interesting result of this study can be related to the formation of monoclinic phase structure of  $\text{La}_{1-x}\text{Sr}_x\text{MnO}_3$  perovskites.

$$\frac{1}{d^2} = \frac{1}{\sin^2 \beta} \left( \frac{h^2}{a^2} + \frac{k^2 \sin^2 \beta}{b^2} + \frac{l^2}{c^2} - \frac{2hl \cos \beta}{ac} \right) \quad (1)$$

$$V = abc \sin \beta \quad (2)$$

### 3.2 Microstructure

The morphology of the obtained lanthanum manganite substitution with different strontium ions content was investigated using field emission electron microscope. **Figure 2** exhibits the FE-SEM micrographs of the samples under study. Evidently, the change in the microstructure was related to the irregular shape of cluster nanoparticles with spherical, spheroidal and polygon morphologies with increasing the  $\text{Sr}^{2+}$  content. Clearly, only LSM powders at low  $\text{Sr}^{2+}$  ratio (0.2) have few aggregates and the average particle size was lower than 100 nm as manifested in **Figure 2a**. Nevertheless, a lot of distinct aggregates was displayed by increasing the  $\text{Sr}^{2+}$  ion content as illustrated in **Figure 2b,c**.

### 3.3 Electro Chemical Impedance Measurements

The electrical behavior of the sample was studied over a wide range of frequency using electrochemical impedance spectroscopy (EIS) technique. This technique enables us to separate the real and imaginary components of the complex impedance and related parameters, and hence provides information of the structure-property relationship of the sample. The polycrystalline



materials usually have grain and grain boundary properties. Therefore, at high temperatures, two successive semicircles may occur due to these properties. These contributions can conventionally be displayed in a complex plane plots (Nyquist and Bode diagram).

**Figure 3** shows the variation of real part of impedance ( $Z'$ ) with frequency at different  $\text{Sr}^{2+}$  ion molar ratios. It is observed that the magnitude of  $Z'$  decreases with the increase in both frequency as well as  $\text{Sr}^{2+}$  ion concentration. This indicates the reduction of grain, grain boundary and electrode interface resistances. The  $Z'$  value for the all substituted samples found to be merged above  $60\text{kHz}$ . The coincidence of the  $Z'$  value at higher frequency side at all samples confirms the concept of space charge effect. This may be due to the release of space charges. The loss spectrum (i.e.  $Z''$  versus frequency) of the compound at the same substitution of  $\text{Sr}^{2+}$  ion molar ratios is given in **Figure 4**. The asymmetric broadening of peaks suggests the presence of electrical process in the material with spread of relaxation time (indicated by peak width). The relaxation species may possibly be due to the presence of electrons/species at lower  $\text{Sr}^{2+}$  ion content and defects/vacancies at high value of  $\text{Sr}^{2+}$ . [Gupta and Mansingh 1994; Behera, Nayak, and Choudhary 2008] The magnitude of existing peaks ( $Z''$ ) decreases gradually with the increase in frequency and  $\text{Sr}^{2+}$  ion substitutions and finally merges in high frequency domain, which indicates the presence of space charge polarization effects at lower frequency and at higher  $\text{Sr}^{2+}$  content. However the frequency dependence of impedance  $Z''$  (loss Spectrum) for LSM at room temperatures is shown in **Figure 4**. It is observed that peaks are found at room temperature. The position of the  $Z''$  peak shifts to higher Frequency side on increasing frequency and then a strong dispersion of  $Z''$  exist.

From **Figure 4**, it is observed that at low frequency region, the  $Z''$  was increased by increasing the  $\text{Sr}^{2+}$  ion content. At the frequency of  $600000\text{Hz}$ , the  $Z''$  have the maximum value

at higher  $\text{Sr}^{2+}$  ion molar ratios of 0.8 Sr. The coincidence of the value of  $Z'$  at higher frequencies at all the  $\text{Sr}^{2+}$  ion content indicates a possible release of space charge (Behera et al. 2013). This may be due to the reduction in barrier properties of the materials with rise in temperature which is responsible for the enhancement of conductivity of the materials (Behera et al. 2013). At a particular frequency,  $Z''$  becomes independent of frequency. This type of behavior is similar to the other material reported by Singh, Kumar, and Yadav (2011). Meanwhile, the peaks of the plot of  $Z''$  decreases gradually with increasing the frequency towards high frequency side, and this is an indication of the accumulation of space charge in the materials (Behera, Nayak, and Choudhary 2007).

### 3.4 The Mott–Schottky Measurements

The Mott–Schottky and  $C-F$  plots at different  $\text{Sr}^{2+}$  ion contents for LSM prepared by co-precipitation method using methylamine as a base and annealed at '1000 °C' for 2h are given in **Figure 5**. The  $C-F$  plot shows a minimum capacitance  $C_{\min}$  at low frequency for all samples. By increasing the frequency range, the capacitance increased to be maximum capacitance at the frequency of 800 KHz. On the other hand, by increasing the Sr ion molar ratios, the capacitance increased from  $4 \times 10^7$  at 0.2  $\text{Sr}^{2+}$  ions to be  $6 \times 10^7$  at 0.5  $\text{Sr}^{2+}$  and to reach at least  $9 \times 10^7$  at 0.8  $\text{Sr}^{2+}$  ion concentrations

## 4 CONCLUSIONS

LSM has been synthesized by a co-precipitation processing using methyl amine as a base at pH 12. Well crystalline monoclinic perovskite like structure of LSM was composed at annealing temperature 1000°C for 2h. The crystallite size was seemed to increase with increment of  $\text{Sr}^{2+}$  ion concentration. Furthermore, the unit cell volume was found to slightly

decrease with enhanced the  $\text{Sr}^{2+}$  content. Meanwhile, the specific electrical impedance was increased by increasing  $\text{Sr}^{2+}$  ion concentration. The Mott–Schottky and  $C-F$  measurements revealed that by increased  $\text{Sr}^{2+}$  ion molar ratios, the charge space capacity was increased at frequency dependence. Hence, the tunability of the electrical properties makes  $\text{La}_{1-x}\text{Sr}_x\text{MnO}_3$  a promising candidate for cathode materials in solid oxide fuel cell. Work is in progress in order to determine the catalytic activity toward oxygen reduction of our LSM material. The results will open a new route for research into SOFCs, and have great significance on the development of SOFCs.

## References

- Behera, A. K., N. K. Mohanty, B. Behera, and P. Nayak. 2013. *Advanced Materials Letters* 4 (2):141.
- Behera, B., P. Nayak, and R. N. P. Choudhary. 2007. *Materials Chemistry and Physics* 106 (2–3):193.
- Behera, B., P. Nayak, and R. N. P. Choudhary. 2008. *Materials Research Bulletin* 43 (2):401.
- Cesario, M. R., D. A. Macedo, R. M. P. B. Oliveira, P. M. Pimentel, R. L. Moreira, and D. M. A. Melo. 2011. *Journal of Ceramic Processing Research* 12 (1):102.
- Gupta, V., and A. Mansingh. 1994. *Physical Review B* 49 (3):1989.
- Huang, Y. Y., J. M. Vohs, and R. J. Gorte. 2005. *Journal of the Electrochemical Society* 152 (7):A1347.
- Im, J., I. Park, and D. Shin. 2011. *Solid State Ionics* 192 (1):448.
- Jorgensen, M. J., and M. Mogensen. 2001. *Journal of the Electrochemical Society* 148 (5):A433.
- Ju, J., J. Lin, Y. Wang, Y. Zhang, and C. Xia. 2016. *Journal of Power Sources* 302:298.
- Kakade, M. B., S. Ramanathan, and P. K. De. 2003. *British Ceramic Transactions* 102 (5):211.
- Liang, F., J. Chen, S. P. Jiang, B. Chi, J. Pu, and L. Jian. 2009. *Electrochemistry Communications* 11 (5):1048.
- Liu, Z., M. Liu, L. Yang, and M. Liu. 2013. *Journal of Energy Chemistry* 22 (4):555.
- Lu, J., Y. Zhang, Z. Lu, X. Huang, Z. Wang, X. Zhu, and B. Wei. 2015. *RSC Advances* 5 (8):5858.
- Marinsek, M., K. Zupan, T. Razpotnik, and J. Macek. 2007. *Materiali in Tehnologije* 41 (2):85.
- Orera, A., and P. R. Slater. 2010. *Chemistry of Materials* 22 (3):675.
- Reshi, H. A., A. P. Singh, S. Pillai, R. S. Yadav, S. K. Dhawan, and V. Shelke. 2015. *Journal of Materials Chemistry C* 3 (4):820.
- Sholklapper, T. Z., V. Radmilovic, C. P. Jacobson, S. J. Visco, and L. C. De Jonghe. 2007. *Electrochemical and Solid State Letters* 10 (4):B74.
- Singh, H., A. Kumar, and K. L. Yadav. 2011. *Materials Science and Engineering: B* 176 (7):540.
- Turky, A. O., M. M. Rashad, and M. Bechelany. *Materials & Design* 90:54–5.

- Turky, A. O., M. M. Rashad, A. M. Hassan, E. M. Elnaggar, and M. Bechelany. 2016. *RSC Advances* 6 (22):17980.
- Turky, A. O., M. M. Rashad, A. E.-H. Taha Kandil, and M. Bechelany. 2015. *Physical Chemistry Chemical Physics* 17 (19):12553.
- Wang, J. X., Y. K. Tao, J. Shao, and W. G. Wang. 2009. *Journal of Power Sources* 186 (2):344.
- Yan, K.-L., R.-H. Fan, Z.-C. Shi, M. Chen, L. Qian, Y.-L. Wei, K. Sun, and J. Li. 2014. *Journal of Materials Chemistry C* 2 (6):1028.
- Yang, X., and J. T. S. Irvine. 2008. *Journal of Materials Chemistry* 18 (20):2349.
- Zhi, M., G. Zhou, Z. Hong, J. Wang, R. Gemmen, K. Gerdes, A. Manivannan, D. Ma, and N. Wu. 2011. *Energy & Environmental Science* 4 (1):139.

**Table 1.** Crystallite size, the lattice constant and the unit cell volume of LSM nanopowders prepared by co-precipitation method at different  $\text{Sr}^{2+}$  ion molar ratios annealed at 1000°C for 2h

Sr <sup>2+</sup> ion content	Crystallite size (nm)	Lattice parameter(Å)			Unit cell volume(Å <sup>3</sup> )
		<i>a</i>	<i>b</i>	<i>c</i>	
0.2	16.4	5.5212	7.8712	5.6421	245.2
0.5	22.6	5.5211	7.8211	5.6411	243.6
0.8	29.3	5.5201	7.8201	5.6400	243.5

**Table 2.** Electrical parameters of LSM nanopowders prepared by co-precipitation method at different  $\text{Sr}^{2+}$  ion molar ratios

Sample ID	$Z' (\Omega)$	$Z'' (\Omega)$	$ Z  (\Omega)$	$1/C (F)$	$1/C^2 (F)$
LSM2	10	10	12	$4.5 \times 10^7$	$2.1 \times 10^{15}$
LSM5	16	14	18	$6.5 \times 10^7$	$4.5 \times 10^{15}$
LSM8	24	22	26	$9.5 \times 10^7$	$9.4 \times 10^{15}$

**Figure 1.** The XRD patterns of Lanthanum strontium manganite nanopowders  $\text{La}_{1-x}\text{Sr}_x\text{MnO}_3$  prepared by co-precipitation method using methylamine as a base at different  $\text{Sr}^{2+}$  ion molar ratios (0.2, 0.5, and 0.8) annealed at  $1000^\circ\text{C}$  for 2h .

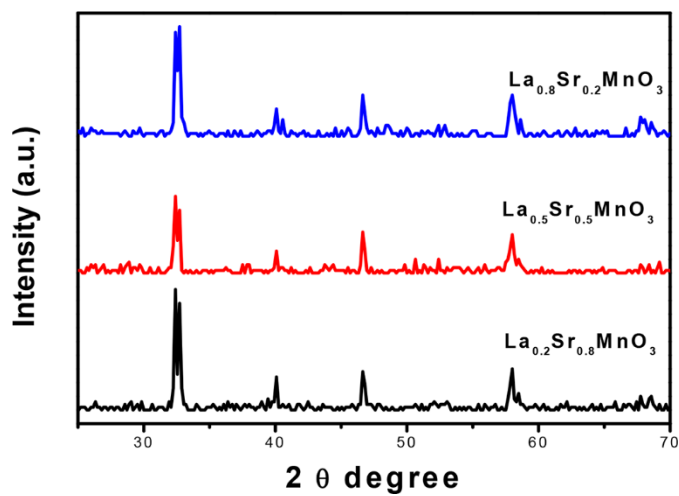


**Figure 2.** SEM image of Lanthanum strontium manganite nanopowders prepared by co-precipitation method with different  $\text{Sr}^{2+}$  ion molar ratios concentration (0.2, 0.5, and 0.8).

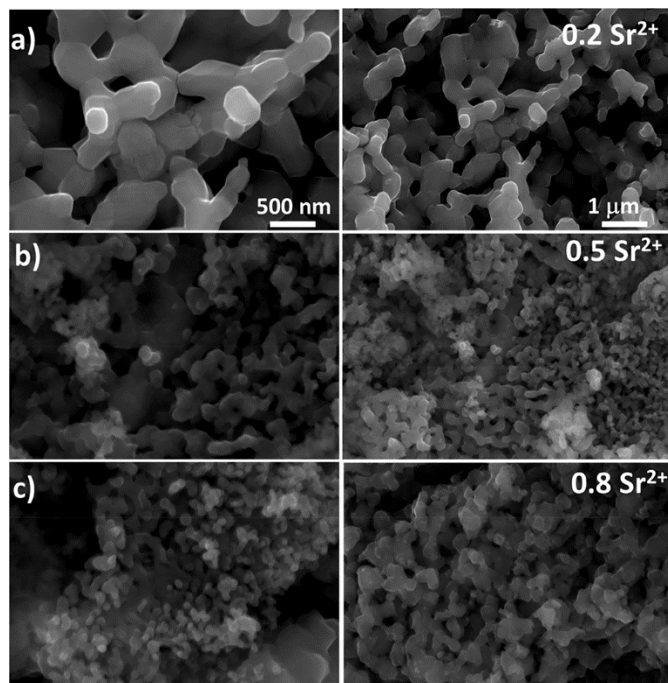




**Figure 3.** Frequency dependence of ( $Z'$ ) part of impedance of LSM prepared by co-precipitation method and thermally treated at '1000 °C' for annealing time of '2 h' with different  $\text{Sr}^{2+}$  ion molar ratios.

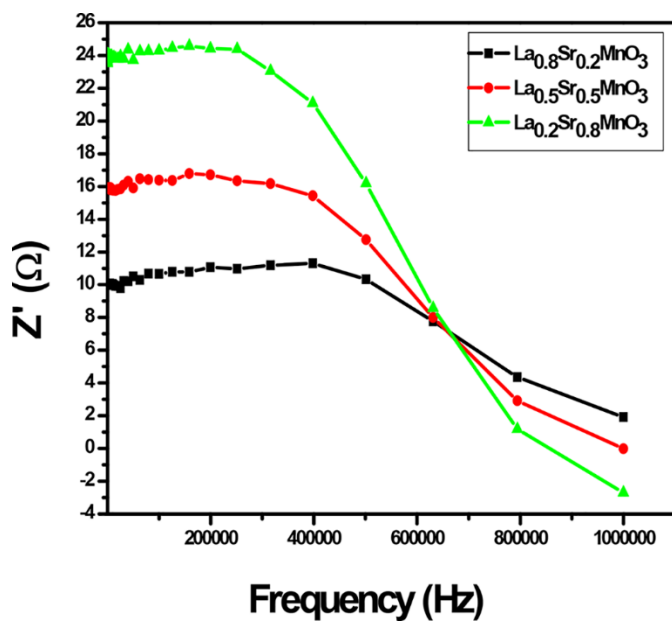


**Figure 4.** Frequency dependence of ( $Z''$ ) part of impedance of LSM prepared by co-precipitation method and thermally treated at '1000 °C' for annealing time of '2 h' with different  $\text{Sr}^{2+}$  ion molar ratios.

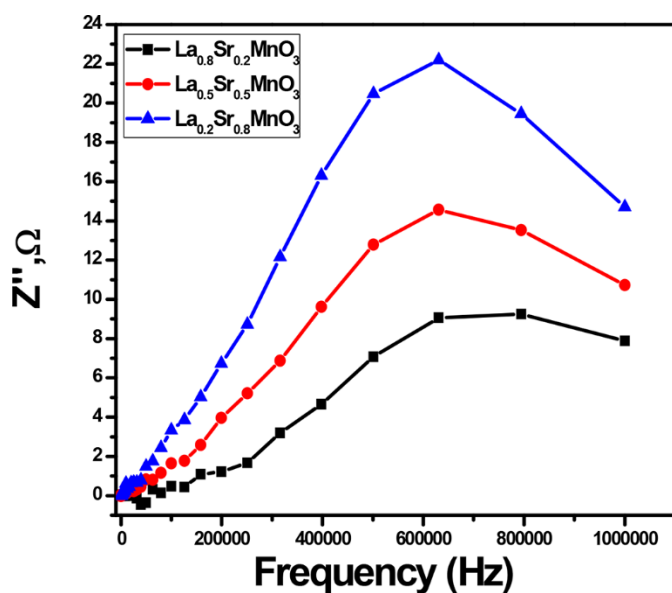


**Figure 5.** The Mott–Schottky ( $C-F$  plots) of LSM prepared by co-precipitation method and thermally treated at ‘1000 °C’ for annealing time ‘2 h’ with different  $\text{Sr}^{2+}$  ion molar ratios.

